# Approximating Anisotropic Paths on Terrains *

Mark Lanthier, Anil Maheshwari,
Jörg-Rüdiger Sack

August 6, 2004

**Abstract**

We discuss the problem of computing shortest an-isotropic paths on terrains. Anisotropic path costs take into account the length of the path traveled, possibly weighted, the direction of travel along the faces of the terrain, and the energy expended due to friction and gravity. Parameters such as the varied nature of the terrain, friction, or slope of each face, can be captured via face weights. Anisotropic paths add realism by taking into consideration the direction of the travel on each face thereby e.g., eliminating paths that are too steep for vehicles to travel and preventing the vehicles from turning over. Prior to this work an $O(n^n)$ time algorithm had been presented for computing anisotropic paths. Here we present the first polynomial time approximation algorithm for computing anisotropic paths. Our algorithm is simple to implement and allows for the computation of anisotropic paths within a desired accuracy. We provide supporting experimental results. Our result addresses the corresponding problem posed in [20].
**Keywords:** *Computational Geometry, Shortest Path, Approximation Algorithm, Anisotropic Paths.*

# 1 Introduction

## 1.1 Motivation and Previous Work

Shortest path problems arise in many application areas and they are among the fundamental problems in computational geometry. In computational geometry objects are often modeled via terrains. A *terrain* is a set of points and edges (connecting them) whose projection onto the $xy$-plane forms a triangulation.

A large body of work has centered around the computation of Euclidean shortest paths (we refer the reader to the survey in [14]). For terrains, Sharir and Schorr [19] presented an algorithm for computing Euclidean shortest paths and now we know of a number of different algorithms (see cf. [1, 2, 14]). Euclidean shortest paths on terrain surfaces may

*Research supported in part by NSERC. School of Computer Science, Carleton University, Ottawa, Canada.

not generally provide optimal time or energy paths since they ignore the terrain attributes. *Weighted shortest paths* (introduced in [13]) provide more realism in that they can incorporate terrain attributes such as variable costs for different regions. This allows one to take into consideration e.g. that the cost of traveling through water, sand, or on a highway is typically different. The NP-hardness and the large time complexities of 3-d shortest paths algorithms even for special problem instances have motivated the search for approximate solutions to the shortest path problem. For weighted shortest path approximations on planar subdivisions or polyhedra, recently, several algorithms have been proposed [1, 2, 3, 4, 5, 10, 18].

In the model introduced by [13], the direction of travel along a face is not captured. The direction of travel plays an important role in determining the physical effects incurred on a vehicle (e.g., car, truck, robot, or even person) traveling along a terrain surface. Through *anisotropism*, we can identify certain directions of travel that represent inclines that are too steep to ascend or unsafe to travel due to possible dangers such as overturning, sliding or wheel slippage. It is for these reasons that we investigate *anisotropic* paths, i.e., paths that take into account the direction of travel as well as length and other physical properties. The model was introduced by Rowe and Ross [15] and it subsumes all previously published criteria for traversal for isotropic weighted region terrain. They present an algorithm which runs in $O(n^n)$ time in the worst case for an $n$-vertex terrain. The high time complexity of this algorithm motivates the study of approximation algorithms for anisotropic shortest path problems. Refer to [14, 15] for applications, further pointers and discussion on regular grid based heuristics for these problems.

The quality of an approximate solution is assessed in comparison to the correct solution. One particular class of approximation algorithms produces $1+\epsilon$-approximations of the shortest path. Since mostly the geographic models are approximations of reality anyway and high-quality paths are favored over optimal paths that are "hard" to compute, approximation algorithms are suitable and necessary. In $1+\epsilon$-approximation algorithms accuracy, arbitrarily high, can be traded off against run-time. Such algorithms are appealing and are thus well studied, in particular, from a theoretical view-point.

## 1.2 New Results

In this paper we address the problem of computing an $1+\epsilon$-approximation $\Pi'(s,t)$ to a shortest anisotropic path $\Pi(s,t)$ for a point vehicle between two points, $s$ and $t$, on a terrain $\mathcal{P}$ with $n$ faces, where $\frac{\|\Pi'(s,t)\|}{\|\Pi(s,t)\|} < 1+\epsilon$, for any given $\epsilon > 0$. The cost of a path $\Pi(s,t)$ is denoted by $\|\Pi(s,t)\|$ and it equals the sum of the weights of the segments constituting the path.

Our approach is to discretize the polyhedral terrain in a natural way, by placing Steiner points along the edges of the polyhedron. We construct a graph $G$ containing the Steiner points as vertices and edges as those interconnections between Steiner points that correspond to segments which lie completely in the triangular faces of the polyhedron. The geometric shortest path problem on polyhedra is thus stated as a graph problem so that the existing efficient algorithms (and their implementations) for shortest paths in graphs can be used. The main difference to [10, 4] and to other somewhat related work (e.g., [5, 6, 8]) lies in the placement of Steiner points, due to the directional restrictions imposed on the path segments

in this case.

We introduce a logarithmic number of Steiner points along each edge of $\mathcal{P}$, and these points are placed in a geometric progression along an edge. They are chosen w.r.t. (i) the vertex joining two edges of a face such that the distance between any two adjacent points on an edge is at most $\epsilon$ times the shortest possible path segment that can cross that face between those two points (ii) eight direction ranges (three impermissible, one braking and four regular) such that the approximation segment is of the same type as that of the shortest path segment.

We show that there exist a path in the graph $G$ with cost that is within $(1 + f(\epsilon))$ times the shortest path costs, where $f(\epsilon)$ is a function of $\epsilon$ and geometric parameters of the terrain. The running time of our algorithm is the cost for computing the graph $G$ plus that of running a shortest path algorithm in $G$.

The paper is organized as follows. In Section 2 we introduce the physical model that is used to determine the cost of an anisotropic path and present properties of shortest anisotropic paths. In Section 3 we describe an $1+\epsilon$-approximation algorithm for computing anisotropic paths. In Section 4 we present experimental results by adapting an implementation presented in [11].

# 2 Model and Anisotropic Paths

## 2.1 Physical Model

We use the model proposed by Rowe and Ross [15] for solving the minimal energy path problem. The model allows two main forces to act against the propulsion of a vehicle, namely friction and gravity. It is assumed that the vehicle has no net acceleration over the path from $s$ to $t$ and that the cost of turning is insignificant with respect to energy loss. Also, the model ignores the cost and feasibility of making turns.

We assume that the terrain surface $\mathcal{P}$ is composed of $n$ triangular faces, each face $f_j, 1 \leq j \leq n$, having a homogeneous weight (cost) $\mu_j$ pertaining to the coefficient of kinetic friction (between 0 and 1) for that face with respect to the moving vehicle.

### 2.1.1 Basic Model: Weight Metric

Let $mg$ be the weight of the vehicle where $m$ is the mass of the vehicle and $g$ is the coefficient of gravity. Consider a segment $s_i$ of a shortest path which crosses a face $f_j$ of $\mathcal{P}$. Let $\phi_j$ be the inclination angle (gradient) of $f_j$ and let $\varphi_i$ be the inclination angle of $s_i$ with respect to the XY plane (see Figure 1). Our model assumes that the terrain has no vertical faces and so it is always the case that $-90 < \phi_j, \varphi_i < 90$. Our model assumes that the cost of travel for $s_i$ is:

$$mg(\mu_j \cos\phi_j + \sin\varphi_i) \cdot |s_i| \tag{1}$$

We assume that $mg$ is constant for the problem instance and hence we will ignore it during the computation of the path and multiply the path cost by this factor after it has been computed. The cost due to the force of friction is represented by $\mu_j \cos\phi_j \cdot |s_i|$. Rowe and

Ross [15] reason about paths in their 2-D azimuth projections on the plane of the terrain. They ignore the $\cos\phi_j$ factor, stating that it is very close to 1 for most traversable natural terrain. We keep this value since it is easily computed and can be combined with the $\mu_j$ factor to get an overall face weight. Therefore, it is convenient to define $w_j = \mu_j \cos\phi_j$ to be the weight of face $f_j$. Let $W$ (respectively $w$) be the maximum (respectively minimum) of all $w_j, 1 \leq j \leq n$. The cost due to gravity is represented by $|s_i| \sin\varphi_i$ which is the change in

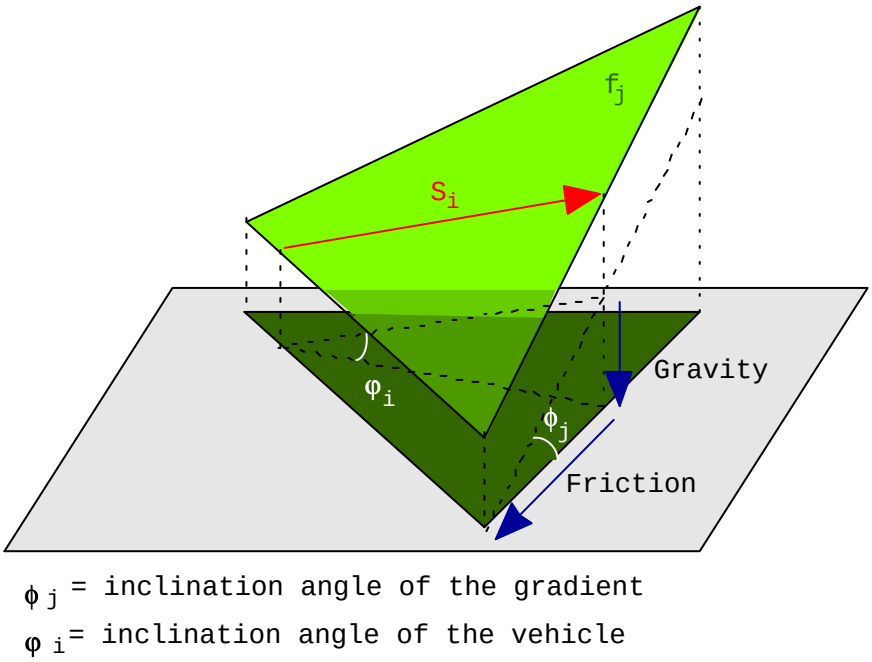


Figure 1: The forces of friction and gravity that act against the propulsion of the vehicle.

elevation of the segment $s_i$. Hence the work expended against gravity during path traversal is merely the sum of the elevation changes of all the path segments. This sum represents the difference in height between $s$ and $t$ which is independent of the path taken. As a result, we can leave this portion out when computing a shortest cost path and add it after the path has been computed.

Note that this model ignores internal energy losses (such as heat loss in an engine), friction of wheels on axles and wind resistance, and costs of turning. Rowe and Ross [15] claim that internal energy losses are proportional to external work done against friction and gravity and can be handled by an appropriate multiplication factor. Also, the wheel friction and wind resistance can be modeled proportional to the path distance.

Consequently, the "uphill" anisotropic cost of travel (i.e., when the cost formula of Equation (1) is positive) for a segment $s_i$ through a face $f_j$ is $w_j|s_i|$. Notice that this cost is the same as that of the weighted isotropic shortest path cost that was used in [4, 2, 11, 13]. We will now consider the effects of braking and invalid directions (obstacles).

### 2.1.2 Model With Braking

For inclination angles $\varphi_i < -\arcsin(\mu_j \cos\phi_j)$, the cost formula of Equation (1) becomes negative, representing an energy gain while going downhill. This however, violates our earlier assumption that there is no net acceleration. We denote the inclination angle $\varphi_i = -\arcsin(\mu_j \cos\phi_j)$ in which this sign change occurs as a *critical braking angle.* To compensate, the cost formula is adjusted so that the energy gained going downhill is exactly compensated by the energy required to brake. So, the vehicle neither accelerates nor does it gain or lose energy when traveling in a braking range. Furthermore, it will be assumed that braking requires negligible energy. The compensation is made possible by replacing the $\mu_j \cos\phi_j$ friction factor by $-\sin\varphi_i$ which cancels out the gravity force resulting in zero cost travel. Notice that although the cost for downhill braking is zero, the negative gravity force has already been extracted from the metric, leaving a cost of $-\sin\varphi_i \cdot |s_i|$ for segment $s_i$. This cost will always be positive and non-zero for the valid range of downhill angles: $-90 < \varphi_i < 0$ degrees. Such a segment is called a *braking* segment and it is always assigned a positive, non-zero weight.

**Property 1** *For a braking segment $s_i$ passing through face $f_j$, $-\sin\varphi_i \geq w_j$.*

**Proof:** For braking segments, $\varphi_i < -\arcsin(\mu_j \cos\phi_j)$. This can be rewritten as $\varphi_i < -\arcsin(w_j)$. Hence $-\sin\varphi_i \geq w_j$.

□

### 2.1.3 Model With Anisotropic Obstacles

One last characteristic of the model is that it will prevent travel in "unsafe" directions. Rula and Nuttall [16] indicate that four conditions can give anisotropic slope limitations:

1. Limited expendable force to counteract friction and gravity effects. Here the traveling inclination angle $\varphi_i$ cannot exceed $\arcsin(\frac{F_{max}}{mg\sqrt{\mu_j^2+1}}) - \arctan(\mu_j)$ where $F_{max}$ is the maximum force that the vehicle can exert.

2. Speed or power limitations of the vehicle. Here the traveling inclination angle $\varphi_i$ cannot exceed $\arcsin(\frac{P_{max}}{v_{min}mg\sqrt{\mu_j^2+1}}) - \arctan(\mu_j)$ where $P_{max}$ is the maximum power that the vehicle can exert and $v_{min}$ is the minimum (non-zero) speed of the vehicle.

3. Loss of traction danger (slippage). This occurs when the traveling inclination angle $\varphi_i$ exceeds approximately $\arctan(\mu'_j - \mu_j)$, where $\mu'_j$ is the coefficient of static friction of face $f_j$.

4. Sideslope overturn danger. Here the projection of the center of gravity falls outside the polygon formed by its support points (most often perpendicular to "uphill"). The formula here depends on the vehicle shape (see Figure 2).

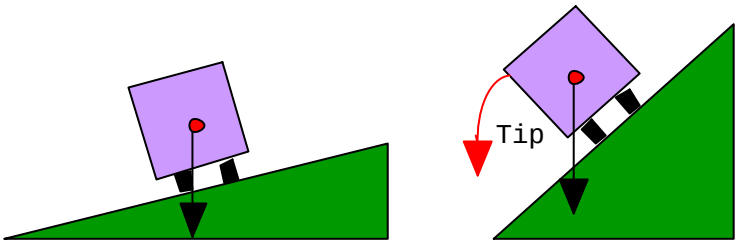


Figure 2: The sideslope overturn problem. The vehicle tips as its center of gravity projection falls outside the support polygon defined by the wheels.

The formulae above give rise to possibly three ranges of angles that define directions on a face that are impermissible for traveling. These are denoted as *impermissible ranges*. Together, with the braking range, there are up to four important angular ranges per face as shown in Figure 3. The boundary angles of the impermissible ranges are called *critical impermissibility angles*. The boundary angles of the braking range are called *critical braking angles*. For the regular angular ranges (i.e., not impermissible or braking), the range is bounded by critical impermissibility or braking angles. These angles will be called the *critical regular angles* for that regular range. Note that in the case of very steep angles, an impermissible range may arise within the braking range due to dangers of wheel slippage. That is, some ranges of downward traversal may be too steep for safe travel. We will ignore this impermissible range, since the face itself should be deemed unsafe for travel anyway. A path is said to be *valid* if and only if it does not travel in any impermissible directions.

If any of the impermissible ranges overlap, they are combined to make a single impermissible range. In some cases, the impermissible ranges may cover all possible angles. This represents an *isotropic obstacle* which is essentially a face that cannot be traveled on safely. If there exists an isotropic obstacle on $\mathcal{P}$ then it is possible that a valid path between two arbitrary points on $\mathcal{P}$ does not exist.

**Property 2** *Given two points $s$ and $t$ on $\mathcal{P}$, there may not be a valid path $\Pi(s,t)$ between them.*

The algorithm description and analysis presented here will assume that there exists at least one valid path, $\Pi(s,t)$ between $s$ and $t$. Although we make this assumption in the analysis, our algorithm is able to detect the absence of valid paths and report when such a path does not exist. All that remains to be shown is that if a valid path does indeed exist, then our algorithm will always produce a valid path as well.

Let $\varphi_c$ be a critical impermissibility angle for one of the critical impermissibility ranges of a face $f_j, 1 < j < n$ of $\mathcal{P}$. Let $\vec{u}$ and $\vec{v}$ be the two unit vectors representing the directions on the boundaries of the range (these are called a *matched pair* of critical angles). Thus, the angle that $\vec{u}$ and $\vec{v}$ make with the horizontal plane is $\varphi_c$. Let $\alpha_c$ be the angle between these two vectors when placed end-to-end as shown in Figure 4. Let $\alpha_j$ be the minimum of all $\alpha_c$ for the (up to three) impermissible ranges of $f_j$. Define $\beta_j, 1 < j < n$ to be the angle

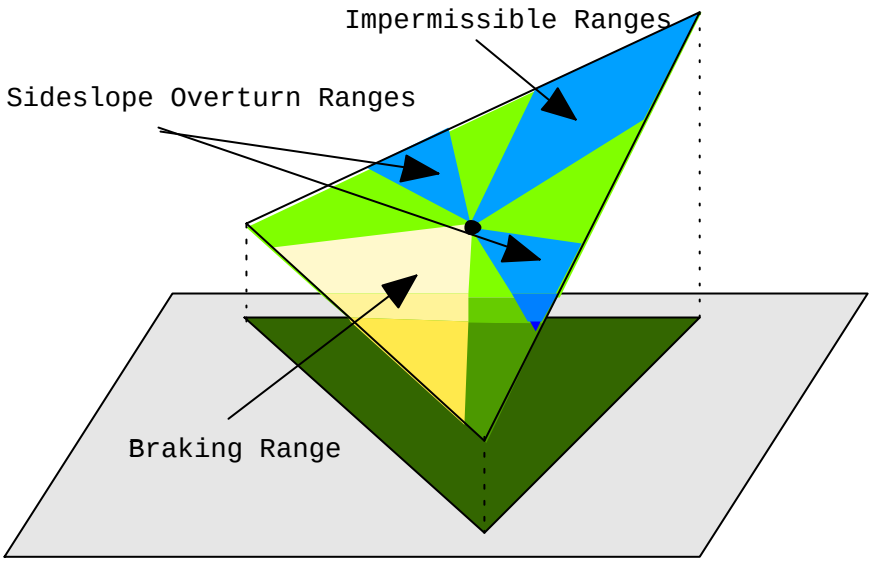


Figure 3: The up to three ranges representing impermissible travel and the braking range with respect to the center point of a single face.

on $f_j$ between the matched pair of braking angles and $\lambda_j, 1 < j < n$ to be the minimum angle on $f_j$ between a matched pair of regular angles on $f_j$. Furthermore, for $1 < j < n$ let $\alpha = \min(\alpha_j)$, $\beta = \min(\beta_j)$, and $\lambda = \min(\beta_j, \lambda_j)$.

## 2.2 Path Types and Properties

On flat terrains, our model behaves like a weighted shortest path as there are no braking or impermissible ranges. That is, the path bends at edges of the terrain, obeying Snell's law of refraction. For non-flat terrains with steep slopes, the path characteristics are different. Rowe and Ross [15] show that a shortest anisotropic path can traverse a face in three different ways as shown in Figure 5. This corresponds to one of three types of face crossings which we denote as *direction types*:

1. *Regular*: Straight across at a permissible non-braking obeying Snell's law along the face boundaries (may travel along a critical angle).

2. *Switchback*: Given a matched pair of critical impermissibility direction vectors $\vec{u}$ and $\vec{v}$, this path consists of consecutive straight line segments that alternate in directions $\vec{u}$ and $\vec{v}$. Each change in direction is called a *switchback*.

3. *Braking*: Straight across with braking at a non-critical heading.

The algorithm of Rowe and Ross [15] computes a shortest energy path for a vehicle moving in a terrain. Their algorithm computes all possible combinations of the three traversal types above at each edge encountered during propagation. They exhaust all possibilities through an $A^*$ search (see [7]) resulting in an $O(n^n)$ algorithm in the worst case. They do however,

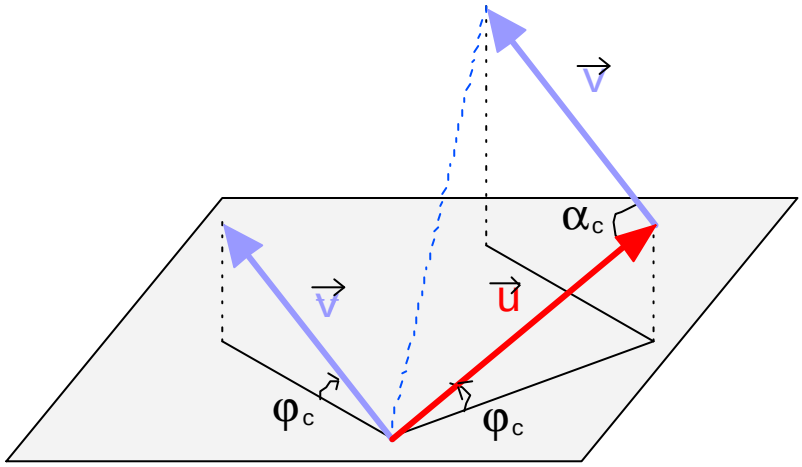


Figure 4: The value of $\alpha_c$ with respect to critical angle vectors $\vec{u}$ and $\vec{v}$.

use a set of heuristics and pruning techniques to help alleviate this large time complexity, stating that it performs much better than this pessimistic bound. In their implementation, switchback paths were disallowed.

Let us examine a switchback path that passes through a face $f_j$. Rowe and Ross [15] show that these switchback paths are contained within $f_j$. Furthermore, they show that a switchback path consists of a chain of consecutive segments directed in the directions of a matched pair of critical impermissibility angle directions. This matched pair of angle directions, say $\vec{u}$ and $\vec{v}$, correspond to the boundaries of a single impermissibility range.

**Property 3** *A switchback path between a point $x$ of $\mathcal{P}$ and a vertex $v$ of $\mathcal{P}$ may have an infinite number of segments.*

Therefore, it is possible that the number of segments in a switchback path could be infinite, but there is a concise description of such paths. In our algorithms, we will therefore treat a switchback path as a single segment and assign a weight to it which incorporates the length of the switchback path itself. This allows us to compute paths with a finite number of segments. The actual path cost is bounded as we will now show.

Let $\vec{u}$ and $\vec{v}$ be the critical angles that define the directions of the switchback path through a face $f_j$. The following properties bound the length of this switchback path between two given points $a$ and $b$ lying in the plane defined by $f_j$:

**Property 4** *There exist real scalars $C_1$ and $C_2$ such that $b = a + C_1\vec{u} + C_2\vec{v}$.*

**Property 5** *There exist real scalars $C_1$ and $C_2$ such that $C_1|\vec{u}| + C_2|\vec{v}| \leq \frac{|\overline{ab}|}{\sin(\alpha_j/2)}$.*

**Proof:** By Property 4, let $c$ be the point at which $(a + C_1\vec{u})$ and $(b - C_2\vec{v})$ meet. Thus, $a, b$ and $c$ form a triangle $\triangle acb$, as shown in Figure 6. Let $\omega = \angle cba, \psi = \angle bac$ and $\alpha_j = \angle acb$.

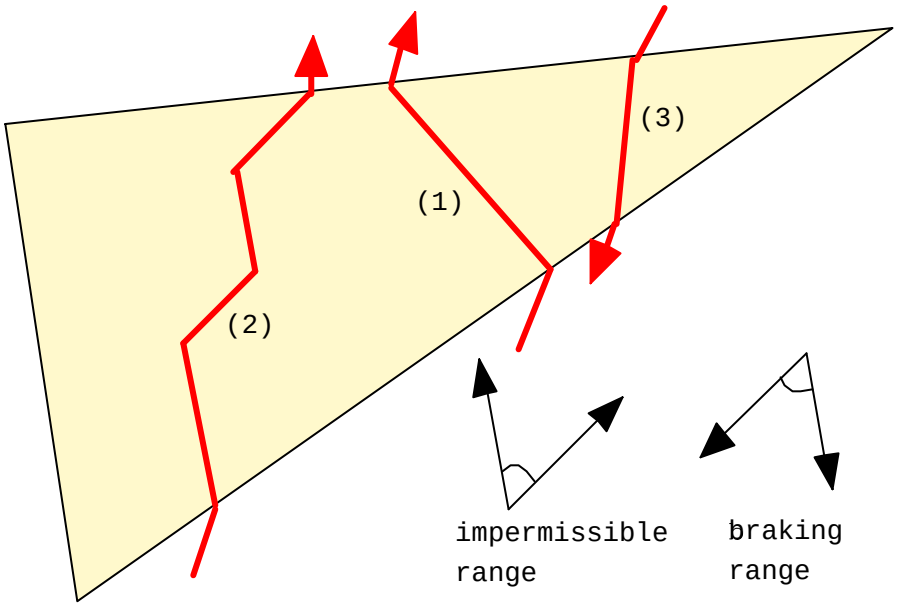


Figure 5: The 4 ways in which a shortest anisotropic path can cross a face.

The sine law ensures that $\sin\omega = \frac{C_1|\vec{u}|\sin\alpha_j}{|\overline{ab}|}$ and that $\sin\psi = \frac{C_2|\vec{v}|\sin\alpha_j}{|\overline{ab}|}$. Thus,

$$C_1|\vec{u}| + C_2|\vec{v}| = \left(\frac{\sin\omega + \sin\psi}{\sin\alpha_j}\right)|\overline{ab}| \tag{2}$$

If $\omega \geq \psi$ then $\sin\frac{\omega}{2} \geq \sin\frac{\psi}{2}$ and $\cos\frac{\omega}{2} - \cos\frac{\psi}{2} \leq 0$. Similarly, if $\omega \leq \psi$ then $\sin\frac{\omega}{2} \leq \sin\frac{\psi}{2}$ and $\cos\frac{\omega}{2} - \cos\frac{\psi}{2} \geq 0$. In either case, $\sin\frac{\omega}{2}\left(\cos\frac{\omega}{2} - \cos\frac{\psi}{2}\right) \leq \sin\frac{\psi}{2}\left(\cos\frac{\omega}{2} - \cos\frac{\psi}{2}\right)$, and so $\sin\frac{\omega}{2}\cos\frac{\omega}{2} + \sin\frac{\psi}{2}\cos\frac{\psi}{2} \leq \sin\frac{\omega}{2}\cos\frac{\psi}{2} + \sin\frac{\psi}{2}\cos\frac{\omega}{2}$ or $\frac{\sin\omega}{2} + \frac{\sin\psi}{2} \leq \sin\left(\frac{\omega+\psi}{2}\right)$. This can be simplified by substituting $\omega + \psi = \pi - \alpha_j$ as follows: $\sin\omega + \sin\psi \leq 2\sin\left(\frac{\pi}{2} - \frac{\alpha_j}{2}\right) \leq 2\cos\frac{\alpha_j}{2}$ $\leq \frac{2\sin\alpha_j\cos\frac{\alpha_j}{2}}{\sin\alpha_j} \leq \frac{\sin\alpha_j}{\sin\frac{\alpha_j}{2}}$. Hence, $\frac{\sin\omega+\sin\psi}{\sin\alpha_j} \leq \frac{1}{\sin\frac{\alpha_j}{2}}$.

□

**Claim 1** *A switchback path between two points $a$ and $b$ on a face $f_j$ which uses directions defined by $\vec{u}$ and $\vec{v}$ has length at most $\frac{|\overline{ab}|}{\sin(\alpha_j/2)}$.*

**Proof:** Given two points $a$ and $b$ on a plane and two non-parallel vectors $\vec{u}$ and $\vec{v}$, it is easy to see that all paths that join $a$ and $b$ and are composed solely of segments that are directed in directions $\vec{u}$ and $\vec{v}$ have the same length. Since switchback paths for a given impermissibility range travel in at most two non-parallel directions, all switchback paths for a given impermissibility range between $a$ and $b$ have equal length. From Property 5, this length is at most $\frac{|\overline{ab}|}{\sin(\alpha_j/2)}$.

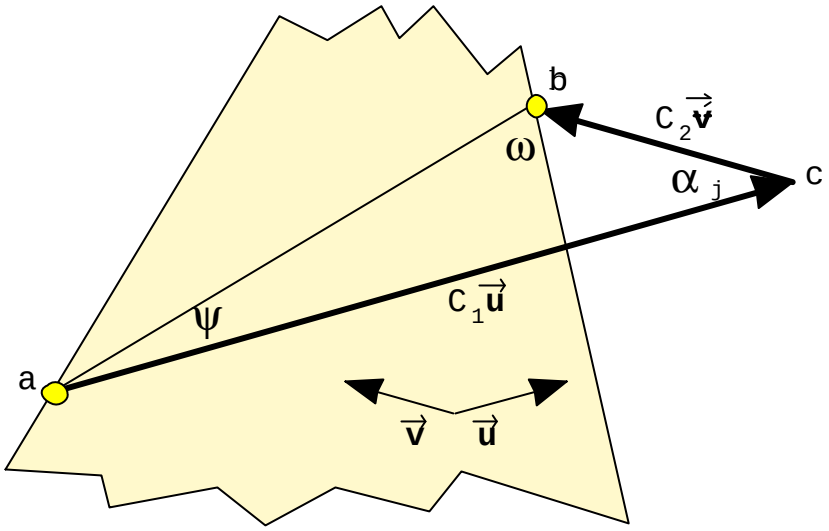


Figure 6: The triangle formed by extending $\vec{u}$ and $-\vec{v}$ from points $a$ and $b$, respectively.

□

**Claim 2** *A shortest anisotropic path $\Pi(s,t)$ is a simple path.*

**Proof:** Consider an edge $\overline{ab}$ of $\Pi(s,t)$ that crosses a face $f_j$ of $\mathcal{P}$. Assume that some other edge $\overline{cd}$ of $\Pi(s,t)$ crosses (i.e., intersects) $\overline{ab}$ at some point $x$ on $f_j$ (e.g., see Figure 7). Clearly, the subsegment $\overline{ax}$ of $\overline{ab}$ is shorter than $\overline{ab}$ and so it would be cheaper to remain at $x$ instead of traveling from $x$ through $b$ along $\Pi(b,c)$ then along $\overline{cx}$. Hence, $\overline{ax}$ and $\overline{cx}$ cannot be on $\Pi(s,t)$ because it would cause a contradiction of $\Pi(s,t)$ being a shortest path. Note that $\vec{cd}$ is a valid direction and so is $\vec{xd}$.

□

Note that Claim 2 is true only because there is no turning constraint at $x$. That is, our model does not consider the cost or feasibility of making turns. If for example, $\angle axd$ represented a turn that was too sharp, it may not be permissible to turn at $x$ and perhaps the path through $b$ and $c$ would be a shortest permissible path from $a$ to $d$.

We will now investigate the number of segments of $\Pi(s,t)$. We use the discretization scheme proposed in [4], where Steiner points are placed outside "small spheres" centered at each vertex. Let $v$ be a vertex of $\mathcal{P}$. Define $h_v$ to be the minimum distance from $v$ to the boundary of the union of its incident faces. Define a polygonal cap $C_v$, called a *sphere*, around $v$, as follows. Let $r_v = \epsilon h_v$ for some $0 < \epsilon$. Let $r$ be the minimum $r_v$ over all $v$. Let $vuw$ be a triangulated face incident to $v$. Let $u'$ (respectively, $w'$) be at the distance of $r_v$ from $v$ on $vu$ (respectively, $vw$). This defines a triangular sub-face $vu'w'$ of $vuw$. The spherical cap $C_v$ around $v$ consists of all such sub-faces incident at $v$. If a segment intersects an edge of $\mathcal{P}$ within some distance $r_v$ of any vertex $v$ then it is called an *inside-sphere* segment. From here on, we will assume that $k$ is finite and each switchback path is considered to be a single

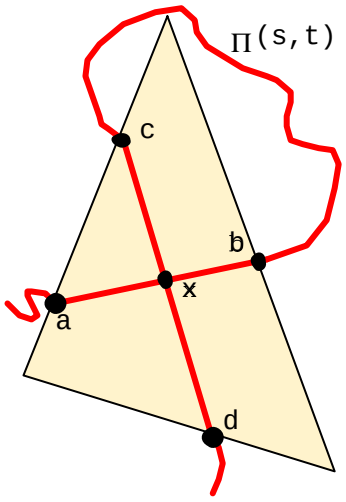


Figure 7: The impossible situation in which an edge $\overline{ab}$ of $\Pi(s,t)$ supposedly intersects another edge $\overline{cd}$ of $\Pi(s,t)$.

segment. Still, the task of bounding $k$ is non-trivial. Instead, we will give a bound for $k^*$, which we denote as the number of non inside-sphere segments of $\Pi(s,t)$. The following claim bounds $k^*$.

**Claim 3** *If $\Pi(s,t)$ does not have any inside-sphere segments then it may cross an edge of $\mathcal{P}$ at most $O(\log_{\mathcal{F}} \frac{|L|}{r})$ times, where $\mathcal{F} = (1 + \min(w, \sin\frac{\alpha}{2})\sin\theta)$.*

**Proof:** See Appendix.

**Lemma 1** *A shortest anisotropic path $\Pi(s,t)$ that does not have any inside-sphere segments can have at most $O(n \log_{\mathcal{F}} \frac{|L|}{r})$ segments, where $\mathcal{F} = (1 + \min(w, \sin\frac{\alpha}{2})\sin\theta)$ and $r$ defines the radius of the smallest sphere around a vertex of $\mathcal{P}$.*

# 3 An $\epsilon$-Approximation

## 3.1 Computing the Graph

We begin by constructing a graph $G_j$ for each face $f_j$ of $\mathcal{P}$ by adding Steiner points along edges of $f_j$ in three stages. In the *first stage*, we add enough Steiner points to ensure that the distance between adjacent Steiner points on an edge is at most $f(\epsilon)$ times the length of a shortest path segment which passes through it, for some function $f(\epsilon)$ which is independent of $n$. This is done using the algorithm of [4]. The *second stage* of Steiner points are required to ensure that there exists an approximation segment with the same direction type as a shortest path segment which passes between the same Steiner points. Recall that our model of computation allows for eight direction ranges per face. Second stage adds a set of Steiner

points to $f_j$ corresponding to the braking range and (up to four) regular ranges. We give here a description of how to add the Steiner points corresponding to the braking range; the Steiner point sets for the regular ranges are constructed in a similar manner. In the *third stage*, we expand $G_j$ by placing additional vertices within at least one of the spheres around a vertex of $f_j$.

### 3.1.1 Stage 1

For each vertex $v$ of face $f_j$ we do the following: Let $e_q$ and $e_p$ be the edges of $f_j$ incident to $v$. First, place Steiner points on edges $e_q$ and $e_p$ at distance $r_v$ from $v$; call them $q_1$ and $p_1$, respectively. By definition, $|\overline{vq_1}| = |\overline{vp_1}| = r_v$. Define $\delta = (1 + \epsilon \sin\theta_v)$ if $\theta_v < \frac{\pi}{2}$, otherwise $\delta = (1 + \epsilon)$. We now add Steiner points $q_2, q_3, ..., q_{\iota_q - 1}$ along $e_q$ such that $|\overline{vq_j}| = r_v \delta^{j-1}$ where $\iota_q = \log_\delta(|e_q|/r_v)$. Similarly, add Steiner points $p_2, p_3, ..., p_{\iota_p - 1}$ along $e_p$, where $\iota_p = \log_\delta(|e_p|/r_v)$.

### 3.1.2 Stage 2

Let $\vec{u}$ and $\vec{v}$ be the critical angle directions for the range on the plane of $f_j$ (see Figure 8). Consider now each vertex $v$ of $f_j$ and apply the following algorithm twice (once as is and then again where $\vec{u}$ and $\vec{v}$ are swapped):

$q \leftarrow v$.
WHILE ($q$ does not lie within $C_{v_i}$ of $f_j$, where $v_i \neq v$) DO {
  $x_q \leftarrow$ the ray from $q$ in direction $\vec{u}$.
  IF ($x_q$ intersects an edge $e$ of $f_j$) THEN {
    $p \leftarrow$ intersection point of $x_q$ and $e$.
    Add $p$ as a Steiner point on $e$.
    $x_p \leftarrow$ the ray from $p$ in direction $-\vec{v}$.
    IF ($x_p$ does not intersect an edge $e$ of $f_j$) THEN STOP
    ELSE {
      $q \leftarrow$ intersection point of $x_p$ with $e$.
      Add $q$ as a Steiner point on $e$. } } }

Note that when applying this stage to the adjacent faces of $f_j$, some additional Steiner points will be added to the edges of $f_j$. When creating the graph for an adjacent face $f_{j+1}$, each edge of $f_j$ may also gain a set of Steiner points due to this second stage construction. Hence, each edge may have two such sets of Steiner points. The first and second stage of Steiner points along with the vertices of $f_j$ become vertices of $G_j$. Connect a pair of vertices in $G_j$ by two oppositely directed edges if and only if 1) they represent Steiner points lying on different edges of $f_j$ or 2) they represent adjacent Steiner points lying on the same edge of $f_j$. In addition, for each vertex of $G_j$ which corresponds to a vertex, say $v$, of $f_j$, connect it with two oppositely directed edges to 1) all vertices of $G_j$ that represent Steiner points lying on the edge opposite to $v$, and 2) the two vertices of $G_j$ corresponding to the two closest Steiner points that lie on the two incident edges of $v$.

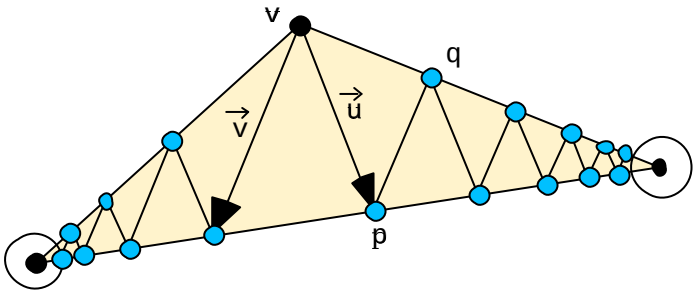


Figure 8: Adding Steiner points to a face corresponding to a braking range.

### 3.1.3 Stage 3

Let $q$ be a Steiner point (or vertex of $f_j$) on edge $e_q$ of $f_j$ which was added during the first or second stage of Steiner placement (including those from adjacent faces as well). Extend rays from $q$ in the directions of $\vec{u}$ and $\vec{v}$. For each ray, if it intersects an edge $e_p \neq e_q$ of $f_j$ at some point $x$ within some $C_v$ of vertex $v$ of $f_j$ then add a Steiner point at $x$. Add $x$ as a vertex of $G_j$ and add edge $\overrightarrow{qx}$ to $G_j$. Also add edge $\overrightarrow{xv}$ to $G_j$. Now extend rays from $q$ in the directions of $-\vec{u}$ and $-\vec{v}$. For each ray, if it intersects an edge $e_p \neq e_q$ of $f_j$ at some point $x$ within a distance of $r_v$ of a vertex $v$ of $f_j$ then add a Steiner point at $x$. Add $x$ as a vertex of $G_j$ and add edge $\overrightarrow{xq}$ to $G_j$. Also add edge $\overrightarrow{vx}$ to $G_j$. Let $q_a$ and $q_{a+1}$ be two adjacent Steiner points added on an edge within a sphere $C_v$ as just mentioned. Let $p_b$ and $p_{b+1}$ be the Steiner points that generated $q_a$ and $q_{a+1}$, respectively. If $|\overline{q_a q_{a+1}}| > r_v(\delta - 1)$ then we add additional evenly spaced Steiner points between $q_a$ and $q_{a+1}$. We add only enough Steiner points to ensure that the distance between two adjacent points is at most $r_v(\delta - 1)$. Once again, connect each of these new Steiner points, say $p$ to $v$ with two oppositely directed edges. Also, connect $p$ to $p_b$ and $p_{b+1}$ with two oppositely directed edges each. Keep in mind that although we just described the addition of these Steiner points with respect to the two critical directions $\vec{u}$ and $\vec{v}$ for the braking range, we must also add similar sets of Steiner points for the regular ranges.

Having added vertices and edges to $G_j$ we must now assign appropriate weights to the edges. For each edge $\overrightarrow{ab}$ of $G_j$, we set its weight as follows: If $\overrightarrow{ab}$ is regular then its weight is set to $w_j|\overline{ab}|$. If $\overrightarrow{ab}$ is braking then its weight is set to $-\sin\theta_i|\overline{ab}|$ where $\theta_i$ is the declination angle of $\overrightarrow{ab}$. If $\overrightarrow{ab}$ is switchback then its weight is set to $\frac{w_j}{\sin\frac{\alpha}{2}}|\overline{ab}|$. This completes the construction of $G_j$. The graph $G$ is defined to be the union $G_1 \cup G_2 \cup \cdots \cup G_n$.

**Claim 4** *$G$ is connected and has $O(n\log_\delta(|L|/r) + n\log_{\mathcal{F}}(r/|L|))$ vertices and $O(n(\log_\delta(|L|/r) + \log_{\mathcal{F}}(r/|L|))^2)$ edges, where $\mathcal{F} = \frac{1+\cos(\theta+\lambda)}{1+\cos(\theta-\lambda)}$, $\theta$ is the minimum angle between any two adjacent edges of any face on $\mathcal{P}$, and $\lambda$ is the minimum of all braking and regular range angles.*

**Proof:** In [4] it is shown that the number of Steiner points added in Stage 1 of the algorithm is $O(n \log_\delta(|L|/r))$. Consider the Steiner points added in Stage 2 of the algorithm. Let $\vec{u}$ and $\vec{v}$ be the two critical angle vectors corresponding to either the braking range or one of the regular ranges of $f_j$. Let $\gamma$ be the angle between $\vec{u}$ and $\vec{v}$. We will examine the creation of Steiner points on two particular edges $e_1$ and $e_2$ of $f_j$. We will bound the number of Steiner points on $e_1$ (as the number of points created on $e_2$ is of the same order). Note that the other ranges will contribute a constant time more Steiner points to $e_1$. Let $v$ be the vertex at the intersection of $e_1$ and $e_2$ such that the angle formed by $e_1$ and $e_2$ in $f_j$ is $\theta$. Let $q_1, q_2, ..., q_\iota$ be the Steiner points added to $e_1$ during Stage 2 of the algorithm such that $q_1$ lies at a distance $r$ from $v$. Let $p_1, p_2, ..., p_{\iota+1}$ be the Steiner points on $e_2$ which were also created during Stage 2 and correspond to the intersection of rays from $q_1, q_2, ..., q_{\iota+1}$, respectively in direction $\vec{u}$ or $\vec{v}$. Let $x_i = \overline{q_{i+1}p_{i+1}}, 0 \leq i \leq \iota$. Let $\sigma = \angle q_i q_{i+1} p_{i+1}$. Let $\delta_0 = |\overline{vq_1}| = r$ and let $\delta_i = |\overline{q_i q_{i+1}}|, 1 \leq i \leq \iota$. Figure 9 illustrates these definitions. We will assume that $\theta_v = \theta$. Furthermore, assume that in the worst case $|e_1| = |L|$. We let $e = e_1$ below to simplify notation. We will determine the length of $\delta_i, 0 < i \leq \iota$ and then determine $\iota$. From the sine

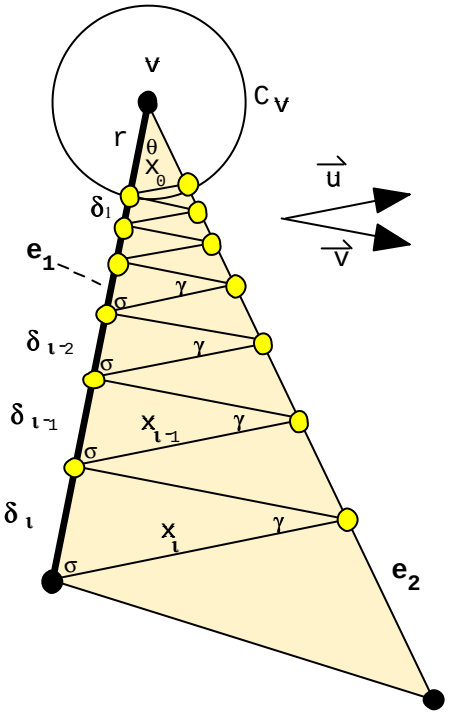


Figure 9: The angles defined during the creation of stage 2 Steiner points for a face $f_j$ based on a single permissible range.

law:

$$\frac{x_\iota}{\sin\theta} = \frac{|e|}{\sin(\pi - (\theta + \sigma))} = \frac{|e|}{\sin(\theta + \sigma)} \tag{3}$$

Hence $x_\iota = \frac{|e|\sin\theta}{\sin(\theta+\sigma)}$. Again using the sine law:

$$\frac{\delta_\iota}{\sin\gamma} = \frac{x_\iota}{\sin(\pi-(\gamma+\sigma))} = \frac{x_\iota}{\sin(\gamma+\sigma)} \tag{4}$$

By combining Equations (3) and (4) we have

$$\delta_\iota = \frac{|e|\sin\theta\sin\gamma}{\sin(\theta+\sigma)\sin(\gamma+\sigma)} \tag{5}$$

Let $\Delta_0 = r$ and $\Delta_i = \delta_0 + \delta_1 + ... + \delta_i$, where $1 \leq i \leq \iota$. By definition, $\Delta_\iota = |e|$. Let $f(\gamma,\theta,\sigma) = \left(\frac{\sin\theta\sin\gamma}{\sin(\theta+\sigma)\sin(\gamma+\sigma)}\right)$. Then, $\Delta_{\iota-i} = \Delta_{\iota-(i-1)} - \delta_{\iota-(i-1)} = |e|(1-f(\gamma,\theta,\sigma))^i$.
In order to bound $\iota$, we would like to find a value for $m$ such that $\Delta_{\iota-m} = \Delta_0 = r$ and so $(1-f(\gamma,\theta,\sigma))^m = \frac{r}{|e|}$. Let $\mathcal{F} = 1-f(\gamma,\theta,\sigma)$, then $m = \log_{\mathcal{F}}\left(\frac{r}{|e|}\right)$. For $\mathcal{F}$ to be a valid base, we need to show that $0 < f(\gamma,\theta,\sigma) < 1$. Clearly, $0 < f(\gamma,\theta,\sigma)$ since $\sigma+\theta+\gamma \leq \pi$ and by a technical proof (see [12]) it follows that $\frac{1}{f(\gamma,\theta,\sigma)} > 1$.

We simplify the expression of $\mathcal{F}$ by placing an upper bound on $\sigma$ and it results in $\mathcal{F} = \frac{1+\cos(\theta+\gamma)}{1+\cos(\theta-\gamma)}$. Since $\gamma$ is defined as the angle between the matched pair of critical angles for a braking or regular range, its minimum value is $\lambda$. This minimal value generates the most Steiner points and will be used as an upper bound for counting the maximum number of Steiner points added during Stage 2. In Stage 3, we add Steiner points in two phases. The first phase adds at most the same order of Steiner points as in Stages 1 and 2 since the new Steiner points are computed by shooting at most two rays from the Steiner points created in Stages 1 and 2. In the second phase we add enough Steiner points to the interior of $C_v$ along $e$ so that the distance between two adjacent points is at most $r_v\epsilon\sin\theta_v$. Hence we add $O(\frac{1}{\delta-1})$ points. By combining the number of Steiner points calculated for Stages 1,2 and 3, we obtain the stated bounds.

□

## 3.2 Constructing the Approximated Path

We describe here the construction of a path $\Pi'(s,t)$ in $G$. In the next section we will bound the cost of this path. Note however that Dijkstra's algorithm may produce a better path than the one constructed here. Recall that a switchback path $z_i$ of $\Pi(s,t)$ within face $f_j$ is represented with a single segment (i.e. $s_i$) of $\Pi(s,t)$ whose weight encapsulates the distance of the switchback path. Each $s_i$, must be of one of the following types:

i) $s_i \cap C_v = \emptyset$,
ii) $s_i \cap C_v =$ subsegment of $s_i$, or
iii) $s_i \cap C_v = s_i$.

Let $C_{\sigma_1}, C_{\sigma_2}, ..., C_{\sigma_\kappa}$ be a sequence of spheres (listed in order from $s$ to $t$) intersected by type ii) segments of $\Pi(s,t)$ such that $C_{\sigma_a} \neq C_{\sigma_{a+1}}$. Now define subpaths of $\Pi(s,t)$ as being one of two kinds:

**Definition 1** Between-sphere subpath: *A path consisting of a type ii) segment followed by zero or more consecutive type i) segments followed by a type ii) segment. These subpaths will be denoted as* $\Pi(\sigma_a, \sigma_{a+1})$ *whose first and last segments intersect* $C_{\sigma_a}$ *and* $C_{\sigma_{a+1}}$*, respectively. We will also consider paths that begin or/and end at a vertex to be a degenerate case of this type of path containing only type i) segments.*

**Definition 2** Inside-sphere subpath: *A path consisting of one or more consecutive type iii) segments all lying within the same* $C_{\sigma_a}$*; these are denoted as* $\Pi(\sigma_a)$*. (Note that inside-sphere subpaths of* $\Pi(s,t)$ *always lie between two between-sphere subpaths. That is,* $\Pi(\sigma_a)$ *lies between* $\Pi(\sigma_{a-1}, \sigma_a)$ *and* $\Pi(\sigma_a, \sigma_{a+1})$*).*

Let $x$ and $y$ be the endpoints of some segment $s_i$ of $\Pi(s,t)$ and let $x$ (respectively $y$) lie on edge $e_q$ (respectively $e_p$) of $f_j$. Let $q_a$ and $q_b$ (respectively $p_a$ and $p_b$) be the Steiner points on $e_q$ (respectively $e_p$) between which $x$ (respectively $y$) lies.

**Claim 5** *At least one of* $\overrightarrow{q_a p_b}$ *or* $\overrightarrow{q_b p_a}$ *is of the same direction type as* $s_i$*.*

**Proof:** Since $s_i$ is an edge of $\Pi(s,t)$, it must travel in either a regular or braking direction. Assume that it is braking and hence we will show that at least one of $\overrightarrow{q_a p_b}$ and $\overrightarrow{q_b p_a}$ is also braking based on the Steiner points added in Stage 2. Let the critical angle directions for this range be $\vec{u}$ and $\vec{v}$. Let $q'_a$ and $q'_b$ be the closest Steiner points to $x$ that were created in Stage 2 from the same range type as $s_i$. Let $p'_a$ and $p'_b$ be the Steiner points that were also created in Stage 2 via the extension of rays from $q'_a$ in the directions $\vec{v}$ and $\vec{u}$, respectively. Similarly, let $p''_a$ and $p''_b$ be the Steiner points that were created in Stage 2 via the extension of a ray from $q'_b$ in the directions $\vec{v}$ and $\vec{u}$, respectively (note that $p'_b = p''_a$). Figure 10 a) and b) show these Steiner points. It may be that $q_a = q'_a$ and/or $q_b = q'_b$. We will assume that these are not equal (as shown in the Figure), although the claim will still hold when either of these are equal. By construction of $G$ during Stage 2, $p_a$ and $p_b$ must lie between either 1) $p'_a$ and $p'_b$ or 2) $p''_a$ and $p''_b$. Consider the first case and extend rays from $q_a$ in the directions of $\vec{v}$ and $\vec{u}$. It is easily seen that $\overrightarrow{q_a p_b}$ lies between these rays and hence is of the same type as $s_i$. Consider now the second case and extend similar rays from $q_b$ to show that $\overrightarrow{q_b p_a}$ lies between these rays as well. Hence, at least one of $\overrightarrow{q_a p_b}$ or $\overrightarrow{q_b p_a}$ is of the same direction type as $s_i$.

□

We begin our path construction by choosing a segment $s'_i$ in $G_j$ which approximates a segment $s_i$ crossing face $f_j$. If $s_i$ is an outside-sphere or overlapping-sphere segment, then choose $s'_i$ to be one of $\overrightarrow{q_a p_a}$, $\overrightarrow{q_a p_b}$, $\overrightarrow{q_b p_a}$ and $\overrightarrow{q_b p_b}$ such that $s'_i$ is of the same direction type as $s_i$ and $\|s'_i\|$ is minimized. Claim 5 ensures that at least one of these segments is of the same type as $s_i$. For the sake of analysis, we will assume that $s'_i$ is chosen so as to have the same direction type as $s_i$ and we will bound $s'_i$ accordingly. In practice however, we may choose a segment with less cost, since we are choosing the minimum of these four. Note that this choice also pertains to the special case in which $e_q = e_p$. Note also that if $s_i$ is an overlapping-sphere segment, then one of $q_a$, $q_b$, $p_a$ or $p_b$ may degenerate to a vertex of

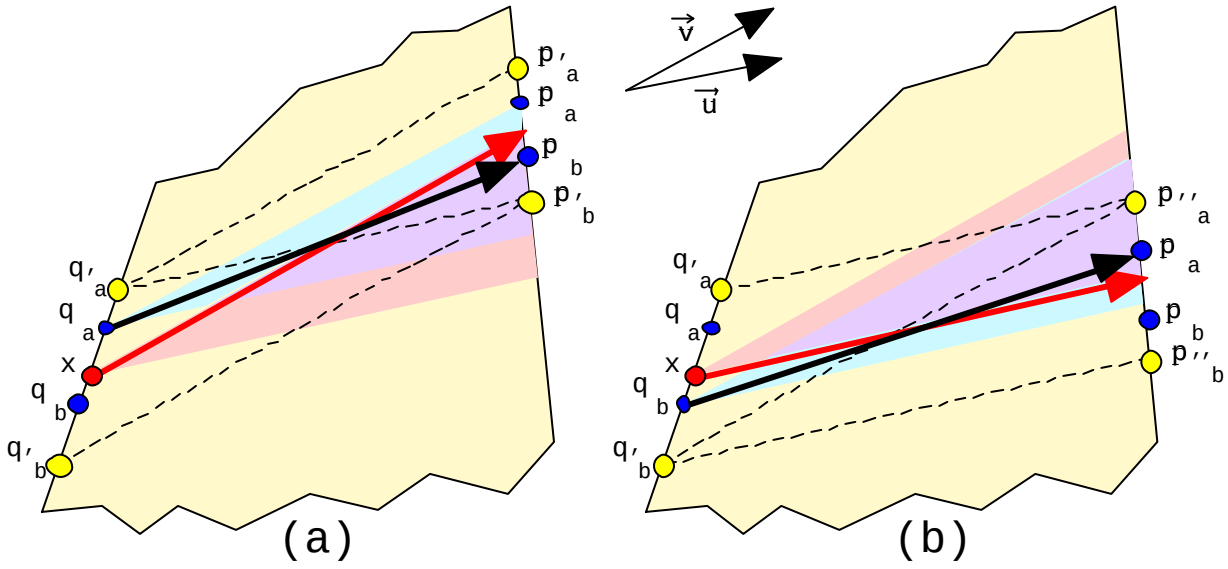


Figure 10: Example showing how $s'_i$ is of the same direction type as $s_i$.

$f_j$. In the case where $s_i$ is an inside-sphere segment, there is no corresponding segment $s'_i$ in $\Pi'(s,t)$.

At this point, we have approximations for all outside-sphere and overlapping-sphere segments but they are disconnected and therefore do not form a path. We will now add edges joining consecutive non-inside-sphere segments $s_i$ and $s_{i+1}$ of $\Pi(s,t)$ with corresponding approximation segments $s'_i$ of $G_j$ and $s'_{i+1}$ of $G_{j+1}$, respectively. Let $e$ be the edge of $\mathcal{P}$ joining faces $f_j$ and $f_{j+1}$. Let $q$ be the endpoint of $s'_i$ lying on $e$ and let $p$ be the endpoint of $s'_{i+1}$ lying on $e$. It is easily seen that either $q = p$ or $q$ and $p$ are adjacent Steiner points on $e$. If $q = p$, then $s'_i$ and $s'_{i+1}$ are already connected. If $q \neq p$ then let $s''_i$ be the edge in $G_j$ from $q$ to $p$. Figure 11 shows two examples of how $s''_i$ is used to connect $s'_i$ and $s'_{i+1}$.

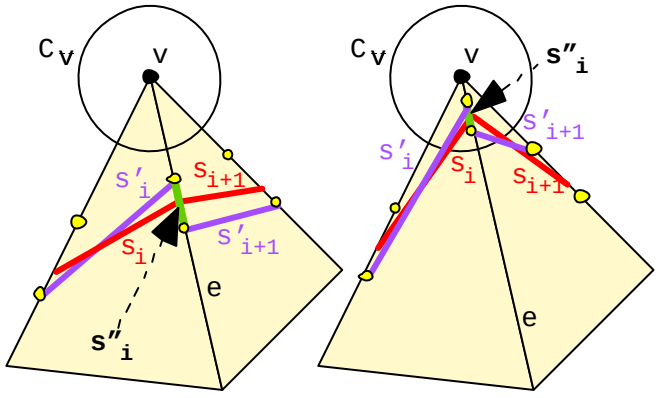


Figure 11: Examples showing the how segments $s'_i$ and $s'_{i+1}$ of $\Pi'(s,t)$ are connected via $s''_i$.

The addition of these segments (i.e., all $s_i''$) ensures that all segments of between-sphere subpaths are connected to form subpaths. We now need to interconnect the between-sphere subpaths so that $\Pi'(s,t)$ is connected.

Consider two consecutive between-sphere subpaths of $\Pi'(s,t)$, say $\Pi'(\sigma_{a-1},\sigma_a)$ and $\Pi'(\sigma_a,\sigma_{a+1})$. They are disjoint from one another, however, the first path ends at a Steiner point within sphere $C_{\sigma_a}$ and the second path starts at a Steiner point within $C_{\sigma_a}$. Join the end of $\Pi'(\sigma_{a-1},\sigma_a)$ and the start of $\Pi'(\sigma_a,\sigma_{a+1})$ to vertex $v_{\sigma_a}$ by two segments (which are edges of $G$ created in Stage 3). These two segments together will form an inside-sphere subpath and will be denoted as $\Pi'(\sigma_a)$. This step is repeated for each consecutive pair of between-sphere subpaths so that all subpaths are joined to form $\Pi'(s,t)$. (The example of Figure 12 shows how between-sphere subpaths are connected to inside-sphere subpaths.) Constructing a path in this manner results in a connected path that lies on the surface of $\mathcal{P}$.

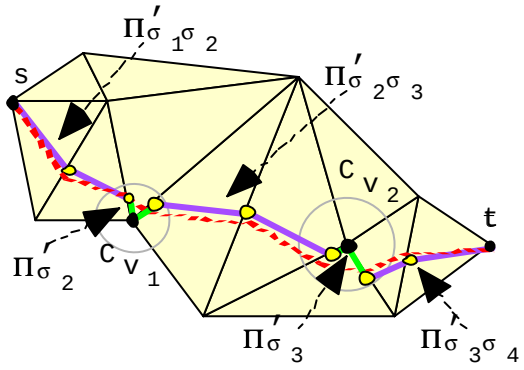


Figure 12: An example showing the between-sphere and inside-sphere subpaths that connect to form the approximated path $\Pi'(s,t)$.

## 3.3 Bounding the Approximation

We give a bound on the cost of $\Pi'(s,t)$. To begin, a bound is shown for each of the between-sphere path segments. The following claim bounds the cost of type i) and type ii) face crossing segments of $\Pi(s,t)$. Assume therefore that $s_i'$ is a type i) or type ii) face-crossing segment. The claim gives bound for the three possible direction types of $s_i'$. That is, we bound the weighted cost of $s_i'$ for the cases in which $s_i'$ (and hence $s_i$) is regular, braking and switchback, respectively. For the following claim, we will assume that $s_i' = \overline{q_a p_b}$; a similar proofs hold when $s_i' = \overline{q_b p_a}$.

**Claim 6** *Let $s_i$ and $s_i'$ be two segments as discussed above, passing through a face $f_j$ which has weight $w_j$. Then*
*i) if $s_i$ and $s_i'$ are regular then $\|s_i'\| \leq (1+2\epsilon)\|s_i\|$*
*ii) if $s_i$ and $s_i'$ are braking then $\|s_i'\| \leq \left(1+\frac{2\epsilon}{w_j}\right)\|s_i\|$.*
*iii) if $s_i$ and $s_i'$ are switchback then $\|s_i'\| \leq \left(1+\frac{2\epsilon}{\sin\frac{\alpha}{2}}\right)\|s_i\|$*
*iv) $\|s_i''\| \leq \frac{\epsilon}{\sin\frac{\alpha}{2}}\|s_i\|$.*

**Proof of Part (i):** Through triangle inequality, we can state that: $|s_i'| \leq |\overline{q_a x}| + |s_i| + |\overline{y p_b}|$. Since Claim 5 ensures that $s_i'$ is indeed regular, then $\|s_i'\| = w_j|s_i'|$ and $\|s_i\| = w_j|s_i|$ and so $\frac{\|s_i'\|}{w_j} \leq |\overline{q_a x}| + \frac{\|s_i\|}{w_j} + |\overline{y p_b}| \leq |\overline{q_a q_b}| + \frac{\|s_i\|}{w_j} + |\overline{p_a p_b}|$.
Since $|\overline{q_a q_b}| \leq \epsilon|s_i|$ and $|\overline{p_a p_b}| \leq \epsilon|s_i|$. Therefore, $\frac{\|s_i'\|}{w_j} \leq 2\epsilon|s_i| + \frac{\|s_i\|}{w_j} = (1+2\epsilon)\frac{\|s_i\|}{w_j}$, and so $\|s_i'\| \leq (1+2\epsilon)\|s_i\|$.
**Proof of Part (ii):** First, examine the maximum possible height difference between $s_i$ and $s_i'$. It is easily seen that $-\sin\varphi_i'|s_i'| \leq -\sin\varphi_i|s_i| + |\overline{q_a q_b}| + |\overline{p_a p_b}|$.
Since Claim 5 ensures that $s_i'$ is braking, we can replace the terms above with the weighted costs $\|s_i'\|$ and $\|s_i\|$. Also we can show that $|\overline{q_a q_b}|$ and $|\overline{p_a p_b}|$ are at most $\epsilon|s_i|$ each. Therefore, $\|s_i'\| \leq \|s_i\| + 2\epsilon|s_i| = \|s_i\| + \frac{2\epsilon\|s_i\|}{-\sin\varphi_i} = (1 + \frac{2\epsilon}{-\sin\varphi_i})\|s_i\|$. The minimum possible value of $-\sin\varphi_i$ is at the critical braking angles (i.e., see Property 1 in which $-\sin\varphi_i = w_j$). Therefore, $\|s_i'\| \leq (1 + \frac{2\epsilon}{w_j})\|s_i\|$.
**Proof of Part (iii):** Figure 13 shows segments $s_i$ and $s_i'$ along with their corresponding switchback paths $z_i = z_{xy}$ and $z_i' = z_{q_a p_b}$. It is easily seen that $|z_{q_a p_b}| = |z_{q_a x}| + |z_{xy}| + |z_{y p_b}|$.

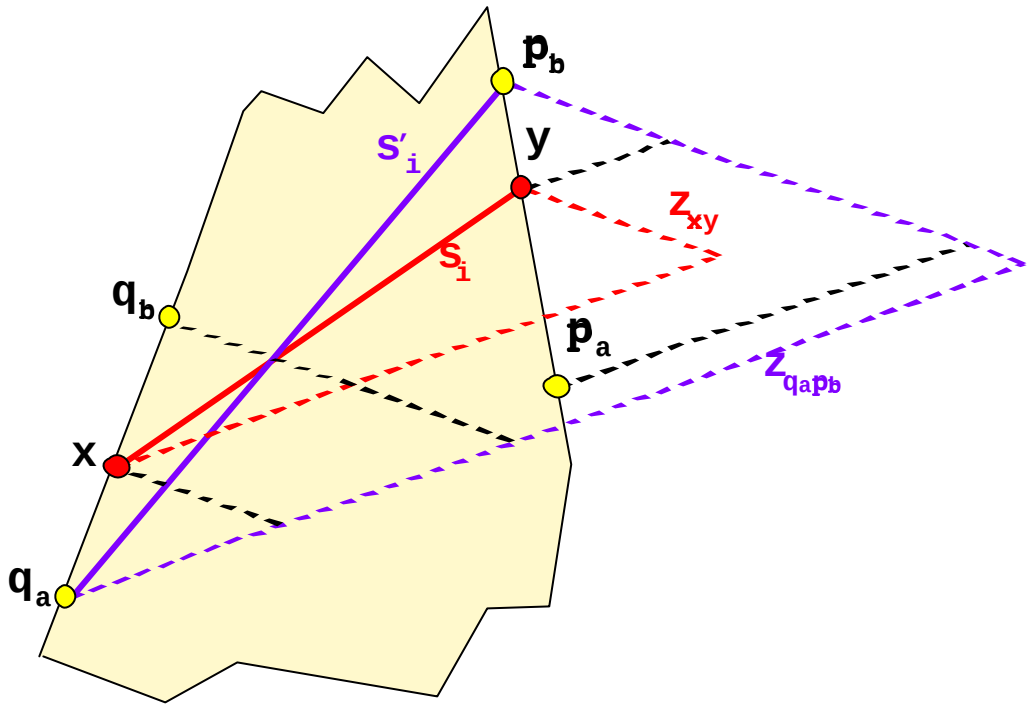


Figure 13: The switchback paths $z_{xy}$ and $z_{q_a p_b}$ corresponding to segments $s_i$ and $s_i'$, respectively.

We upper bound $|z_{q_a x}|$ and $|z_{y p_b}|$ as follows: $|z_{q_a p_b}| \leq |z_{q_a q_b}| + |z_{xy}| + |z_{p_a p_b}| \leq \frac{|\overline{q_a q_b}|}{\sin\frac{\alpha}{2}} + |z_{xy}| + \frac{|\overline{p_a p_b}|}{\sin\frac{\alpha}{2}}$. Since $|\overline{q_a q_b}| \leq \epsilon|\overline{xy}|$ and $|\overline{p_a p_b}| \leq \epsilon|\overline{xy}|$, we obtain $|z_{q_a p_b}| \leq \frac{|\overline{xy}|}{\sin\frac{\alpha}{2}}\epsilon + |z_{xy}| + \frac{|\overline{xy}|}{\sin\frac{\alpha}{2}}\epsilon = \frac{2|\overline{xy}|}{\sin\frac{\alpha}{2}}\epsilon + |z_{xy}| \leq \frac{2|z_{xy}|}{\sin\frac{\alpha}{2}}\epsilon + |z_{xy}| = \left(1 + \frac{2\epsilon}{\sin\frac{\alpha}{2}}\right)|z_{xy}|$. Now $\|s_i'\| = w_j|z_{q_a q_b}|$ and $\|s_i\| = w_j|z_{xy}|$ so $\frac{\|s_i'\|}{w_j} \leq \left(1 + \frac{2\epsilon}{\sin\frac{\alpha}{2}}\right)\frac{\|s_i\|}{w_j}$ and it leads to $\|s_i'\| \leq \left(1 + \frac{2\epsilon}{\sin\frac{\alpha}{2}}\right)\|s_i\|$.

**Proof of Part (iv):** By definition, $s_i''$ joins adjacent Steiner points on an edge of $\mathcal{P}$. Hence, it follows that $|s_i''| \leq \epsilon |s_i|$. It may be that $s_i''$ is impermissible, resulting in $\|s_i''\| \leq \frac{w_j}{\sin\frac{\alpha}{2}}|s_i''|$. Thus,

$$\|s_i''\| \leq \frac{w_j \epsilon}{\sin\frac{\alpha}{2}}|s_i|. \tag{6}$$

If $s_i$ is regular or switchback, then $|s_i| \leq \frac{\|s_i\|}{w_j}$. If $s_i$ is braking, then $|s_i| = \frac{\|s_i\|}{-\sin\varphi_i} \leq \frac{\|s_i\|}{w_j}$. Thus, $|s_i| \leq \frac{\|s_i\|}{w_j}$. Making this substitution into Equation 6 results in $\|s_i''\| \leq \frac{w_j\epsilon}{\sin\frac{\alpha}{2}}\frac{\|s_i\|}{w_j} = \frac{\epsilon}{\sin\frac{\alpha}{2}}\|s_i\|$.

□

**Lemma 2** *If $\Pi'(\sigma_{a-1}, \sigma_a)$ is a between-sphere subpath of $\Pi'(s,t)$ corresponding to an approximation of $\Pi(\sigma_{a-1}, \sigma_a)$ then $\|\Pi'(\sigma_{a-1}, \sigma_a)\| \leq (1+\max(\frac{1}{\sin\frac{\alpha}{2}} + \frac{2}{w}, \frac{3}{\sin\frac{\alpha}{2}})\epsilon)\|\Pi(\sigma_{a-1}, \sigma_a)\|$, where $w$ is the minimum weight of the faces of $\mathcal{P}$.*

Proof: Let $s_i'$ be a segment of $\Pi'(\sigma_{a-1}, \sigma_a)$ which approximates a segment $s_i$ of $\Pi(\sigma_{a-1}, \sigma_a)$ passing through face $f_j$. By Claim 6 we have $\|s_i'\| \leq (1 + 2\epsilon\max(\frac{1}{w}, \frac{1}{\sin\frac{\alpha}{2}}))\|s_i\|$. We can charge the cost of each $s_i''$ to $s_i'$. Therefore, we can say from Claim 6(iv) that $\|s_i'\| + \|s_i''\| \leq (1 + \max(\frac{1}{\sin\frac{\alpha}{2}} + \frac{2}{w}, \frac{3}{\sin\frac{\alpha}{2}})\epsilon)\|s_i\|$. Hence, each segment $s_i'$ of $\Pi'(\sigma_{a-1}, \sigma_a)$ has cost at most $(1+\max(\frac{1}{\sin\frac{\alpha}{2}}+\frac{2}{w}, \frac{3}{\sin\frac{\alpha}{2}})\epsilon)\|s_i\|$ and $\|\Pi'(\sigma_{a-1}, \sigma_a)\| \leq (1+\max(\frac{1}{\sin\frac{\alpha}{2}}+\frac{2}{w}, \frac{3}{\sin\frac{\alpha}{2}})\epsilon)\|\Pi(\sigma_{a-1}, \sigma_a)\|$.

□

**Claim 7** *Let $\Pi'(\sigma_{a-1}, \sigma_a)$ be a between-sphere subpath of $\Pi'(s,t)$ corresponding to an approximation of $\Pi(\sigma_{a-1}, \sigma_a)$ then $\|\Pi'(\sigma_a)\| \leq \left(\frac{2W\epsilon}{w(1-2\epsilon)\sin\frac{\alpha}{2}}\right)\|\Pi(\sigma_{a-1}, \sigma_a)\|$, where $0 < \epsilon < \frac{1}{2}$.*

**Proof:** The distance between $C_{\sigma_{a-1}}$ and $C_{\sigma_a}$ must be at least $(1-2\epsilon)h_{v_{\sigma_a}}$. Since $\Pi(\sigma_{a-1}, \sigma_a)$ is a between-sphere subpath, it intersects both $C_{\sigma_{a-1}}$ and $C_{\sigma_a}$. Thus $|\Pi(\sigma_{a-1}, \sigma_a)| \geq (1-2\epsilon)h_{v_{\sigma_a}}$. By definition, $\Pi'(\sigma_a)$ consists of exactly two segments which together have length satisfying $|\Pi'(\sigma_a)| \leq 2r_{v_{\sigma_a}} = 2\epsilon h_{v_{\sigma_a}}$. Thus, $|\Pi'(\sigma_a)| \leq \frac{2\epsilon}{1-2\epsilon}|\Pi(\sigma_{a-1}, \sigma_a)|$. In the worst case, we can assume that segments of $\Pi'(\sigma_a)$ are impermissible and that $\Pi(\sigma_{a-1}, \sigma_a)$ is braking. Hence, $\|\Pi'(\sigma_a)\| \leq \frac{W}{\sin\frac{\alpha}{2}}|\Pi'(\sigma_a)| \leq \frac{2W\epsilon}{w(1-2\epsilon)\sin\frac{\alpha}{2}}\|\Pi(\sigma_{a-1}, \sigma_a)\|$.

□

**Lemma 3** *If $\Pi(s,p)$ is a shortest anisotropic path in $\mathcal{P}$, where $s$ is a vertex of $\mathcal{P}$ and $p$ corresponds to a vertex of $G$ then there exists an approximated path $\Pi'(s,p) \in G$ such that $\|\Pi'(s,p)\| \leq (1 + f(\epsilon))\|\Pi(s,p)\|$ where $0 < \epsilon < \frac{1}{2}$ and $f(\epsilon) = \left(\epsilon\left(\frac{2W\epsilon}{w(1-2\epsilon)\sin\frac{\alpha}{2}} + \max\left(\frac{1}{\sin\frac{\alpha}{2}} + \frac{2}{w}, \frac{3}{\sin\frac{\alpha}{2}}\right)\right)\right)$.*

**Proof:** Using the results of Claim 7 and Lemma 2, it can be shown that
$\|\Pi'(\sigma_{a-1}, \sigma_a)\| + \|\Pi'(\sigma_a)\| \leq \left(1 + \epsilon\left(\frac{2W\epsilon}{w(1-2\epsilon)\sin\frac{\alpha}{2}} + \max\left(\frac{1}{\sin\frac{\alpha}{2}} + \frac{2}{w}, \frac{3}{\sin\frac{\alpha}{2}}\right)\right)\right)\|\Pi(\sigma_{a-1}, \sigma_a)\|$.
This essentially "charges" the length of an inside-sphere subpath to a between-sphere subpath. The union of all such subpaths form $\Pi'(s,p)$. This allows us to approximate $\Pi'(s,p)$ within the bound of $1+\epsilon\left(\frac{2W\epsilon}{w(1-2\epsilon)\sin\frac{\alpha}{2}} + \max\left(\frac{1}{\sin\frac{\alpha}{2}} + \frac{2}{w}, \frac{3}{\sin\frac{\alpha}{2}}\right)\right)$ times the total cost of all the between-sphere subpaths of $\Pi(s,p)$. Since $\Pi(s,p)$ has cost at least that of its between-sphere subpaths, the lemma holds true.

□

**Theorem 1** *Let $\mathcal{P}$ be a polyhedral surface with maximum and minimum face weights $W$ and $w$, respectively such that $W \geq \sin\frac{\alpha}{2}$, where $\alpha$ is the minimum angle defined by any pair of matched critical impermissible and braking angles. Let $\Pi(s,t)$ be a shortest weighted path on $\mathcal{P}$, where $s$ and $t$ are vertices of $\mathcal{P}$ then there exists an approximated path $\Pi'(s,t) \in G$ such that $\|\Pi'(s,t)\| \leq (1+f(\epsilon))\|\Pi(s,t)\|$, where $f(\epsilon) = \frac{3W\epsilon}{w\sin\frac{\alpha}{2}}$. Moreover, $\|\Pi'(s,t)\|$ can be computed by running Dijkstra's shortest path algorithm on the graph computed in Claim 4.*

# 4 Experimental Results

Results of our experiments in [11] and [12] showed that the algorithm is practical, requiring only a few Steiner points to be added per edge in order to obtain good path accuracy and running time. In this paper we presented an algorithm which, from an implementation perspective, differed primarily in the weights assigned to each edge of the graph and in the particular Steiner point placement. In order to validate its practicality, we performed tests with various terrains using a constant number of Steinerpoints per edge. We explain these tests and the results obtained.

The implementation is based on the code of the algorithm in [11] and [12]. However, with this new implementation, the direction of each edge of the graph is important. Each graph edge is assigned two weights, one for upward traversal and one for downward traversal. Costs are assigned according to the direction range in which the edge is directed (i.e., impermissible, braking or regular). Dijkstra's algorithm is used to compute shortest paths. The purpose of the tests were to determine whether or not similar convergence in accuracy can be obtained as the number of Steiner points added is increased and also to investigate the effect on run time as these points are added. The tests were performed on four of the terrains that were used in [11] and [12]: the 10,082 face terrain, the 5,000 face terrain with random heights, the Madagascar terrain and the North America terrain.

The tests were run by varying the number of Steiner points per edge from 0 to 16. The tests were also performed for various impermissibility angles. That is, different critical impermissibility angles of 5, 10, 15, 30, 45, 60 and 90 degrees were used throughout the tests. The coefficient of static friction for each face was set to one and remained a constant throughout the experiments. Also, the sideslope overturn ranges were not considered throughout the tests. As with our previous work, we ran tests for 100 pairs of randomly selected source and destination vertices and computed the average path cost and average computation time for all the tests.

The graphs of Figure 14 show the convergence behavior of the path accuracy for the different numbers of Steiner points and impermissibility angles. The graphs show that the path cost decreases with an increase in the number of Steiner points per edge of the terrain. Notice however that in some cases, more than six Steiner points are necessary before the convergence occurs. Recall that the 90 degree tests have no impermissibility angles and so the results there are comparable to our weighted isotropic shortest path results of [11] and [12]. As the impermissibility angle decreases, we notice that the path cost also increases. This is because a decrease in impermissibility angle causes a larger impermissibility range

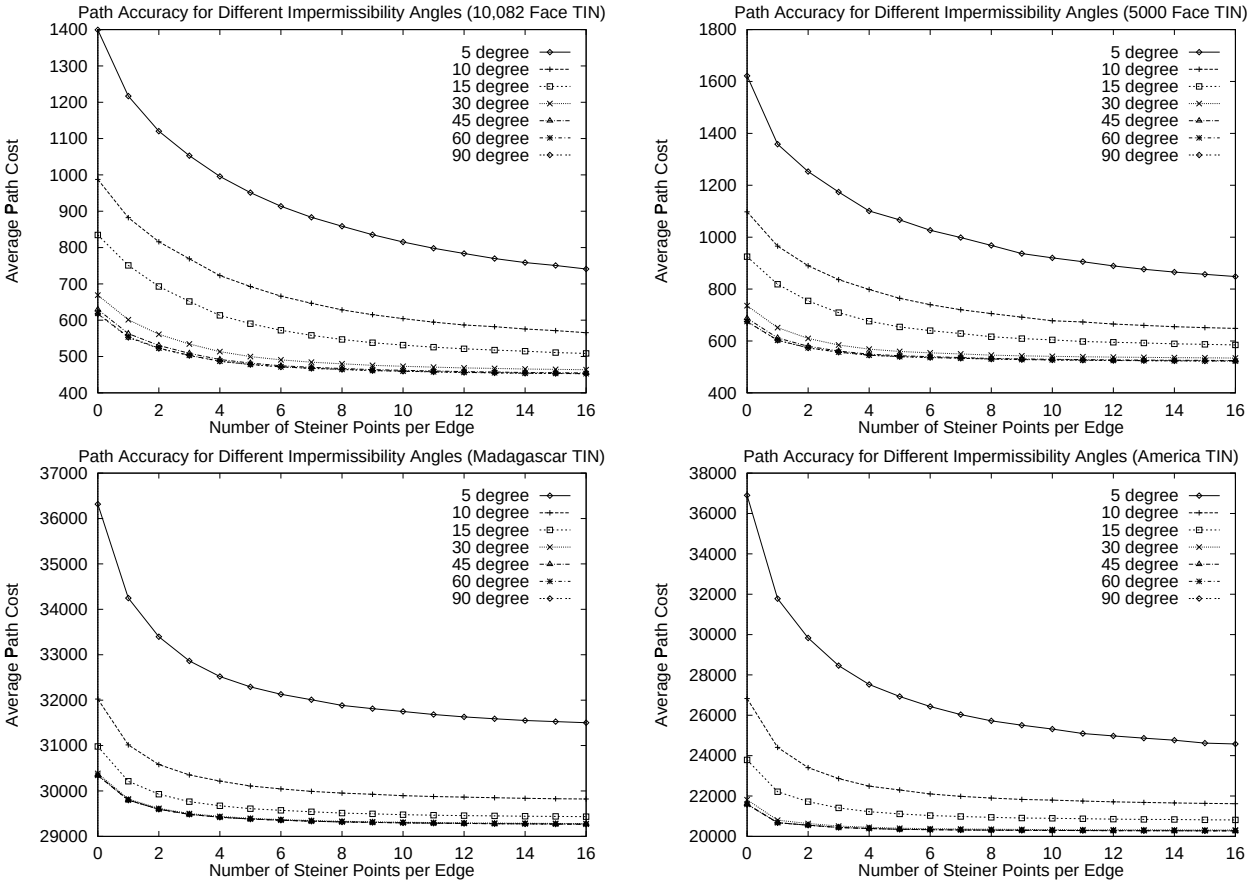


Figure 14: Graphs showing average path cost for four terrains.

and hence more switchback paths are required. Also noticeable is the slower convergence with the smaller impermissibility angles. The switchback paths in a face do not make use of the Steiner points. Therefore, increasing the number of Steiner points on an edge, has no impact on the cost of a particular switchback path within a face. With the larger impermissibility ranges, the path produced by the algorithm has more switchback paths within it and so a high percentage of path segments are unable to make use of the increase in the number of Steiner points.

The graphs of Figure 15 show the average computation time for computing the shortest path costs for the 100 pairs of source/destination vertices. Notice that the graphs exhibit quadratic growth as the number of Steiner points is increased. Also notice that there is no noticeable difference in time between the tests with small or large impermissibility ranges.

The results of our experiments indicate that the algorithm is most practical when impermissibility angles are large. With the larger ranges, only a few Steiner points (i.e., six) are necessary to achieve accurate paths. According to the results of Rula and Nuttall [16], most terrain becomes untraversable when the inclination angle exceeds 30 degrees. On the other hand, 5 degree inclinations are commonly traversable by even the simplest vehicles (i.e., bicycles) without requiring switchbacks. The more realistic values of inclinations that could cause switchbacks are likely between 10 and 30 degrees. By looking at the accuracy graphs of Figure 14, it can be seen that the convergence is better in this range than the 5 degree angle. With additional experimental testing, it is likely that the optimal number of Steiner points to be used may be a function of the impermissibility angles, which in turn depend on vehicle-specific information.

# 5 Conclusions

We presented an algorithm for computing an $1+\epsilon$-approximation to a shortest anisotropic path on the terrain. A similar, but simplified methodology allows for the computation of an approximation to within an additive factor of the shortest anisotropic path (see [12]). Both algorithms expand on and generalize edge subdivision schemes we had introduced earlier [4]. Thus one general technique gives rise to Euclidean, weighted and anisotropic path algorithms. The differences are not so significant for the implementation as they are for the analysis. All graph construction schemes are easy to implement and then require only running a shortest path algorithm. We believe that the approximations within an additive factor will be of special interest for practitioners.

The results detailed here were first presented, as conference version, in [9]. As mentioned in this paper that they are based on the discretization obtained in [11, 4]. These discretization schemes have been subsequently improved in [1, 2] and they require introduction of much fewer Steiner points. Based essentially on the concepts introduced in this paper, Sun and Reif [17] proposed a faster algorithm for approximating anisotropic paths, and the improvements are as follows: (i) they use the discretization schemes proposed in [4, 1], (ii) in place of using Dijkstra's shortest path algorithm, they use the BUSHWHACK algorithm proposed in [18], and (iii) they show that Steiner points added in Stage 1 (see Section 3.1) are sufficient to achieve $1+\epsilon$-approximation.

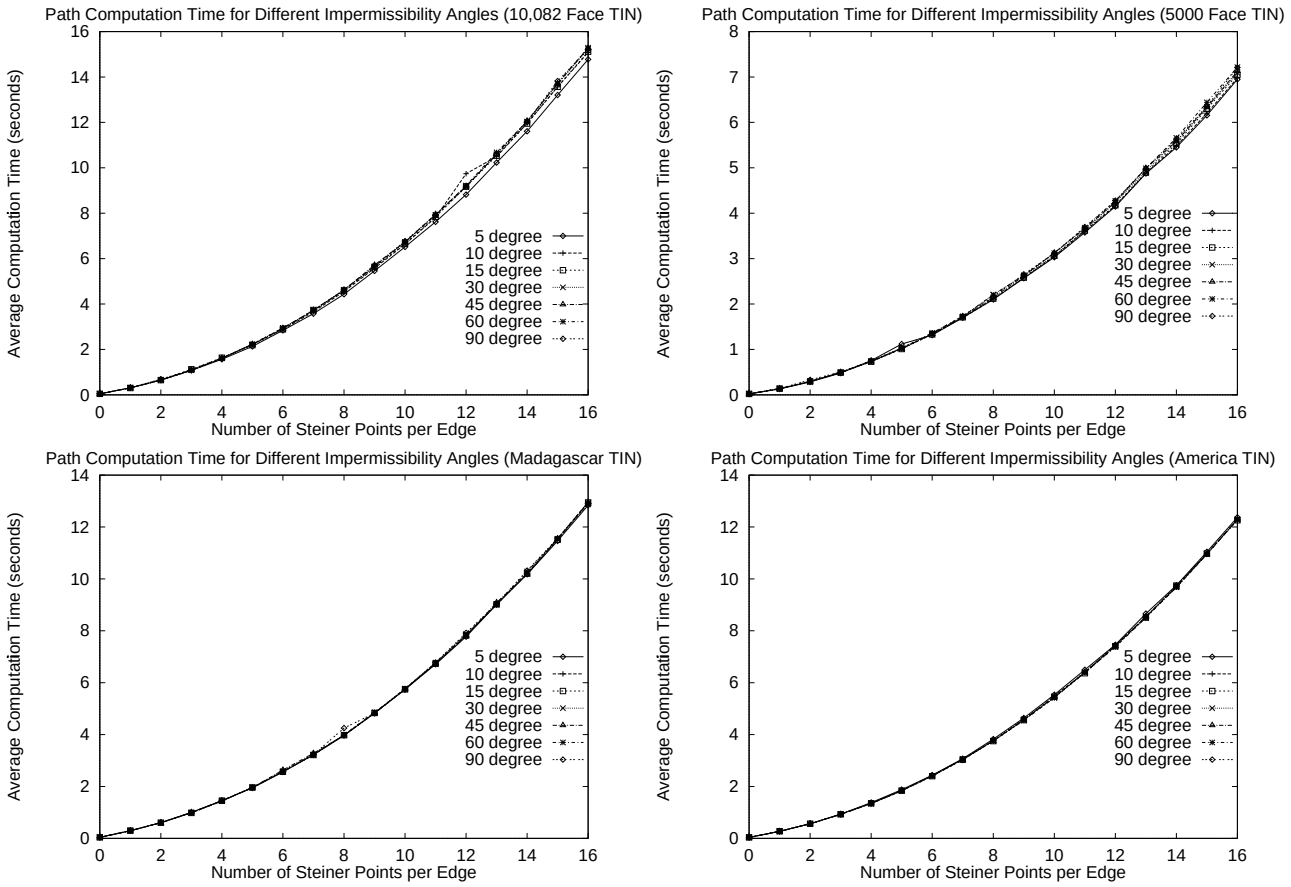


Figure 15: Graphs showing average path computation time for four terrains.

There are a number of questions that still remains to be answered. First of all does the model really captures the reality? (For example, we did not take into account the turning constraints in this work.) The algorithms proposed here as well as that of [17] depend upon the geometric parameters, since the size of the underlying discretization is governed by these parameters. Is it possible to devise an approximation algorithm that is independent of the geometric parameters? This question remains open for the weighted region problem as well.
**Acknowledgments:** The authors would like to thank Lyudmil Aleksandrov for helpful discussion on Claim 4.

# References

[1] L. Aleksandrov, A. Maheshwari and J.-R. Sack, *Approximation algorithms for geometric shortest path problems*, Proc. 32nd ACM Symposium on Theory of Computing, Portland (Oregon), May 2000, pp. 286-295.

[2] L. Aleksandrov, A. Maheshwari and J.-R. Sack, *Approximation algorithms for geometric shortest path problems*, To appear in Journal of ACM.

[3] L. Aleksandrov, M. Lanthier, A. Maheshwari and J.-R. Sack, "An $\epsilon$-Approximation Algorithm for Weighted Shortest Path Queries on Polyhedral Surfaces", *14th European Workshop on Computational Geometry*, Barcelona, Spain, 1998.

[4] L. Aleksandrov, M. Lanthier, A. Maheshwari and J.-R. Sack, "An $\epsilon$-Approximation Algorithm for Weighted Shortest Paths on Polyhedral Surfaces", *SWAT '98*, LNCS 1432, Stockholm, Sweden, 1998, pp. 11-22.

[5] J. Choi, J. Sellen and C.K. Yap, "Approximate Euclidean Shortest Path in 3-Space", *Proc. 10th Annual Symp. on Computational Geometry*, 1994, pp. 41-48.

[6] G. Das and G. Narasimhan, "Short Cuts in Higher Dimensional Space", *Proceedings of the 7th Annual Canadian Conference on Computational Geometry*, Québec City, Québec, 1995, pp. 103-108.

[7] P.E. Hart, N.J. Nilsson, B. Raphael, "A Formal Basis for the Heuristic Determination of Minimum Cost Paths", *IEEE Transactions on System Science and Cybernetics*, SSC-4(2), 1968, pp. 100-107.

[8] C. Kenyon and R. Kenyon, "How To Take Short Cuts", *Discrete and Computational Geometry*, Vol. 8, No. 3, 1992, pp. 251-264.

[9] M. Lanthier, A. Maheshwari and J.-R. Sack, *Shortest anisotropic paths in terrains*, 26th ICALP, LNCS 1644: 524–533, Prague, July 1999.

[10] M. Lanthier, A. Maheshwari and J.-R. Sack, "Approximating Weighted Shortest Paths on Polyhedral Surfaces", *Proceedings of the 13th Annual ACM Symposium on Computational Geometry*, 1997, pp. 274-283.

[11] M. Lanthier, A. Maheshwari and J.-R. Sack, "Approximating Weighted Shortest Paths on Polyhedral Surfaces", *Algorithmica* 30 (4): 527-562, 2001 (Special issue on Algorithmic Engineering). 1999.

[12] M. Lanthier, "Shortest Path Problems on Polyhedral Surfaces", Ph.D Thesis, School of Computer Science, Carleton University, 1999.

[13] J.S.B. Mitchell and C.H. Papadimitriou, "The Weighted Region Problem: Finding Shortest Paths Through a Weighted Planar Subdivision", *Journal of the ACM*, **38**, January 1991, pp. 18-73.

[14] J.S.B. Mitchell, "Geometric Shortest Paths and Network Optimization", in J.-R. Sack and J. Urrutia Eds.,*Handbook on Computational Geometry*, Elsevier Science B.V., to appear 1999.

[15] N.C. Rowe, and R.S. Ross, "Optimal Grid-Free Path Planning Across Arbitrarily Contoured Terrain with Anisotropic Friction and Gravity Effects", IEEE Transactions on Robotics and Automation, Vol. 6, No. 5, October 1990, pp. 540-553.

[16] A.A. Rula and C.J. Nuttall, "An Analysis of Ground Mobility Models(ANAMOB)", *Technical Report M-71-4*, U.S. Army Engineer Waterways Experiment Station, Vicksburg, MS, July 1971.

[17] Z. Sun and J. H. Reif, *On Energy-minimizing Paths on Terrains for a Mobile Robot*, Proc. of IEEE International Conference on Robotics and Automation (ICRA2003), pages 3782-3788, Taipei, Taiwan, Sep. 14-19 2003.

[18] Z. Sun and J. H. Reif, *BUSHWHACK: An approximation algorithm for minimal paths through pseudo-Euclidean spaces*, ISAAC2001, LNCS 2223: 160-171, Christchurch, New Zealand, 2001.

[19] M. Sharir and A. Schorr, "On Shortest Paths in Polyhedral Spaces", *SIAM Journal of Computing*, **15**, 1986, pp. 193-215.

[20] R. Tamassia et al., "Strategic Directions in Computational Geometry", ACM Computing Surveys, Vol. 28, No. 4, December 1996.

## Proof of Claim 3.

Consider a single permissible segment $s_i = \overline{ab}$ of $\Pi(s,t)$ that crosses through a face $f$ of $\mathcal{P}$ where $1 < i < k$. If another segment, say $s_{i+j} = \overline{cd}$, of $\Pi(s,t)$ crosses $f$, then $\angle abc$ and $\angle abd$ must either both be left turns or both be right turns since Claim 2 does not permit $s_i$ and $s_{i+j}$ to cross. Without loss of generality, we will assume that $\angle abc$ and $\angle abd$ are left turns. Let $x_i$ be the segment of minimum cost crossing $f$ with one endpoint at $a$. Without loss of generality assume that $x_i$ is a perpendicular and that it has minimal cost (i.e., smaller of braking or regular cost). Let $e$ be the edge of $f$ on which $a$ lies. We would like to determine a point $a'$ on $e$ such that subsegment $e_a = \overline{aa'}$ of $e$ has cost which is equal to $\|x_i\|$. Clearly $s_{i+j}$ cannot cross $e_a$ (i.e., point $c$ cannot lie on $e_a$) since it would have been cheaper to travel from $a$ to $c$ along $e_a$ than to travel along $s_i$ then along $\Pi(b,c)$. We therefore must ensure that $\|\overline{aa'}\| = \|x_i\|$. The determination of $a'$ gives an indication

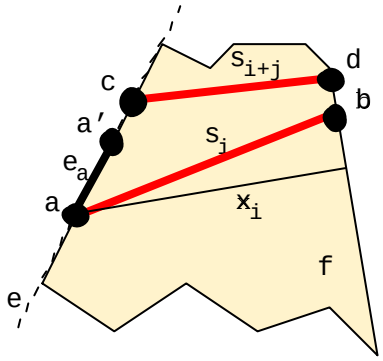


Figure 16: A subsegment $e_a$ which can be crossed by only one segment of $\pi(s,t)$.

as to how close to $a$ another path segment may cross $e$. We then set $a = a'$ and repeat the procedure to obtain a new subsegment $e_{a'}$ along $e$ with respect to $a'$. By continuing in this manner and ensuring that each such subsegment is minimized, we are essentially determining the maximum number of times that $\Pi(s,t)$ can cross edge $e$ (and hence also face $f$ with an additional factor of at most three: pairing of edges).

Due to the different costs that can arise because of the braking and impermissibility ranges we must consider each of the different direction types for $x_i$ and $\overline{aa'}$. For each case we consider the minimum allowable cost of $\overline{aa'}$ in order to get an upper bound on the number of subsegments on $e$.

Let $\varphi_{e_a}$ and $\varphi_{x_i}$ be the inclination angles of $\overline{aa'}$ and $x_i$, respectively. Iterating through all nine cases in which $\overline{aa'}$ and $x_i$ are regular, braking or switchback, it can easily be shown that the smallest possible value of $|\overline{aa'}|$ such that $|\overline{aa'}|$ is maximized is when $|\overline{aa'}| = F|x_i|$, where

$F = \min(1, \frac{-\sin\varphi_{x_i}}{w_f}, \frac{1}{\sin\frac{\alpha}{2}}, \frac{w_f}{-\sin\varphi_{e_a}}, \frac{-\sin\varphi_{x_i}}{-\sin\varphi_{e_a}}, \frac{w_f}{-\sin\varphi_{e_a}\sin\frac{\alpha}{2}}, \sin\frac{\alpha}{2}, \frac{-\sin\varphi_{x_i}\sin\frac{\alpha}{2}}{w_f}, 1)$.

Note that Property 1 ensures that for all terms in the above expression corresponding to braking angles (i.e., when $-\sin\varphi_{e_a}$ or $-\sin\varphi_{x_i}$ are used) then both $-\sin\varphi_{e_a}$ and $-\sin\varphi_{x_i}$ are greater than $w_f$. With the additional fact that $1 \leq \frac{1}{\sin\frac{\alpha}{2}}$ then we can simplify the above

expression to $F = \min(\frac{w_f}{-\sin\varphi_{e_a}}, \sin\frac{\alpha}{2})$. Therefore, $|\overline{aa'}| = \min(\frac{w_f}{-\sin\varphi_{e_a}}, \sin\frac{\alpha}{2})|x_i|$. We can simplify this further by allowing $|\overline{aa'}|$ to be smaller that what is stated here. Note that this change leads to a slightly worse bound on the number of times the edge may be crossed. The simplification is to replace $-\sin\varphi_{e_a}$ by its highest value of 1:

$$|\overline{aa'}| = \min(w_f, \sin\frac{\alpha}{2})|x_i| \tag{7}$$

In order to determine the maximum number of times $e$ may be crossed by $\Pi(s,t)$, we will consider the shortest such subsegments $e_a$ that can be formed along the edge $e$ based on Equation (7). Let $v$ be a vertex of $e$ and let $p_1$ be the intersection point of $C_v$ and $e$. Let $p_2, p_3, p_4, ..., p_\kappa$ be a set of points along $e$ such that

$$|\overline{p_j p_{j-1}}| = (1 + \min(w_f, \sin\frac{\alpha}{2})\sin\theta_v)|\overline{p_{j-1}p_{j-2}}|$$

where $2 < j \leq \kappa$. The value of $\kappa$ represents the limit on the number of points that we can place along $e$ in this fashion. The maximum value of $\kappa$ represents the situation in which $e$ is crossed the most by segments of $\Pi(s,t)$. With a little algebra, it can be shown that $\kappa = O(\log_{\mathcal{F}} \frac{|e|}{r})$, where $\mathcal{F} = (1 + \min(w_f, \sin\frac{\alpha}{2})\sin\theta_v)$. By substituting the worst case when $w_f = w$, $\theta_v = \theta$ and $|e| = |L|$ we obtain the stated bounds.

□